FATIGUE CRACK GROWTH BEHAVIOR OF WC-Co AND WC-CoNi CEMENTED CARBIDES

J. M. Tarragó[1,2 *], J. J. Roa[1,2], V.Valle[1], J. M. Marshall[3], A.Mateo[1], L. Llanes[1,2]

[1] CIEFMA, Departament de Ciència dels Materials i Enginyeria Metal·lúrgica, Universitat Politècnica de Catalunya, ETSEIB, Avda. Diagonal 647, 08028Barcelona, Spain
[*] e-mail: jose.maria.tarrago@upc.edu

[2]CRnE, Centre de Recerca en Nanoenginyeria, Universitat Politècnica de Catalunya, Barcelona 08028, Spain

[3] Sandvik Hyperion, Coventry CV4 0XG, UK

RESUMEN

En este trabajo se investigó el crecimiento de grietas por fatiga para diversas calidades de metal duro en función de la microestructura y el cociente de carga aplicada (R). De esta forma, se evaluó la influencia de la naturaleza química y el contenido del ligante (Co and $76_{wt\%}$Co-$24_{wt\%}$Ni), así como del tamaño de grano de la fase cerámica, en el umbral (K_{th}) y en la cinética de la propagación de grietas por fatiga. Los resultados experimentales indican que las calidades con carburos gruesos presentan un mayor K_{th} que aquellas con un tamaño de grano medio. Esta mejora se asocia con la operatividad del mecanismo de deflexión de grieta. Los resultados señalan que los carburos cementados con base CoNi exhiben una dureza algo inferior que las calidades con base cobalto, pero a su vez presentan valores de tenacidad ligeramente superiores. Por otro lado, la resistencia a la flexión y la sensibilidad a la fatiga no se ven afectadas por la naturaleza química del ligante para los materiales estudiados. Finalmente, se realizó una inspección detallada de la interacción grieta-microestructura, mediante el uso de técnicas de microscopía electrónica de barrido y de difracción de electrones retrodispersados, con el objetivo tanto de evaluar la tortuosidad de la grieta como de discernir los micromecanismos de fatiga en la fase ligante.

ABSTRACT

In this work, the fatigue crack growth (FCG) behavior for several cemented carbides (hardmetal grades) is investigated as a function of microstructure and load ratio (R). In doing so, the influence of binder chemical nature and content (Co and $76_{wt\%}$Co-$24_{wt\%}$Ni), and carbide grain size on FCG threshold (K_{th}) and FCG kinetics is evaluated. Experimental results indicate that coarse-grained grades exhibit higher K_{th} values than medium-grained ones. This improvement is associated with prominence of crack deflection mechanisms. Results show that CoNi-base hardmetals exhibit slightly lower hardness, and higher toughness values than Co-based grades. On the other hand, transverse rupture strength and fatigue sensitivity values are found to be rather independent of the binder chemical nature for the studied materials. Finally, a detailed inspection of crack-microstructure interaction was conducted, by means of field emission scanning electron microscopy and electron backscatter diffraction, in order to evaluate crack path tortousity and to discern fatigue micromechanisms within the metallic binder.

KEYWORDS: Fatigue crack growth, cemented carbides, crystal orientation maps, crack deflection.

1. INTRODUCCTION

The total or partial replacement of cobalt by alternative binders is one of the majors trends in hardmetals industry [1]. Main incentives driven this purpose are toxicity of cobalt, performance improvement under severe working conditions (such as corrosion and high temperature), simpler manufacturing techniques as well as cobalt price increase and fluctuation [1,2]. Accordingly, understanding the microstructure-property relationship of alternative binder hardmetals becomes critical for its proper development.

Fatigue is a relevant service degradation phenomenon in hardmetals and is associated with premature and unexpected failure. Although the first information on the strength degradation of cemented carbides under cyclic loads dates from 1941 [3], the more relevant scientific and technical advances on this field are concentrated in the last twenty years. Among them, it is

noteworthy the findings reported by Sockel's [4–7] and Llanes [8–10] groups, developed following different testing approaches: applied stress – fatigue life (S-N curves) and Fatigue Crack Growth (FCG) tests, respectively. Schleinkofer and co-workers documented a strong strength degradation of cemented carbides under cyclic loads that predominantly occur in the ductile binder phase [4–6] and established that subcritical crack growth is the controlling stage for fatigue failure in cemented carbides [4–7]. On the other hand, Torres and co-workers proposed FCG threshold as the effective toughness under cyclic loading [8]. Moreover, they pointed out that fatigue sensitivity of hardmetals is significantly dependent on its microstructure, according to the compromising role of the binder as the main toughening and fatigue susceptible agent in cemented carbides [9]. This binder fatigue degradation, also observed in the experimental S-N data published by Sailer and co-workers [11], was rationalized on the basis of fatigue-induced accumulation of fcc to hcp phase transformation within the Co binder [4]. As a consequence, the use of binders with distinct chemical nature (e.g. Ni-containing ones) was proposed as a possibility for decreasing the fatigue sensitivity of hardmetals. Thus, it is the aim of this investigation to study the influence of the binder chemical nature and content (Co and $76_{wt\%}$Co-$24_{wt\%}$Ni) on the FCG behavior of cemented carbides. Additionally, microstructural coarsening effects on FCG response, on the basis of carbide grain size, is also investigated.

2. MATERIALS AND METHODS

The investigated materials were WC-Co and WC-CoNi cemented carbides supplied by Sandvik Hard Materials. Eight grades corresponding to different combinations of binder chemical nature, binder content and grain size were studied. The designations and key microstructural parameters: binder content (Wt.%), mean grain size (d_{WC}), carbide contiguity (C_{WC}), and binder mean free path (λ_{binder}) are listed in **Table 1**. Mean grain size was measured following the linear intercept method using a JEOL-7001F field emission scanning electron microscopy (FE-SEM) micrographs. Carbide contiguity and binder mean free path were deduced from best-fit equations, attained after compilation and analysis of data published in the literature (e.g. [12,13]), on the basis of empirical relationships given by Roebuck and Almond [14] but extending them to include carbide size influence [15,16].

Mechanical characterization includes hardness (HV30), transverse rupture strength (TRS), fracture toughness (K_{Ic}) and fatigue crack growth (FCG) parameters. Hardness was measured using a Vickers diamond pyramidal indenter and applying a load of 294N. In all the others cases, testing was conducted using a four-point bending fully articulated test jig with inner and outer spans of 20 and 40 mm respectively. Flexural strength tests were performed on an Instron 8511 servohydraulic machine at room temperature. At least 15 specimens of 45x4x3 mm dimensions were tested per grade. The surface which was later subjected to the maximum tensile loads was polished to mirror-like finish and the edges were chamfered to reduce their effect as stress raisers. Results were analyzed using Weibull statistics. Fracture toughness and FCG parameters were determined using 45x10x5 mm single edge pre-cracked notch beam (SEPNB) specimens with a notch length-to-specimen width ratio of 0.3. Compressive cyclic loads were induced in the notched beams to nucleate a sharp crack and details may be found elsewhere [17]. The sides of SEPNB specimens were polished to follow stable crack growth by a direct-measurement method using a high-resolution confocal microscope. Fracture toughness was determined by testing SEPNB specimens to failure at stress-intensity factor load rates of about 2 MPa√m/s. FCG behavior was assessed for two different load ratio (R) values, 0.1 and 0.5, using a RUMUL resonant testing machine at load frequencies around 150 Hz.

A detailed analysis of crack-microstructure interaction was carried out by means of FE-SEM and electron backscatter diffraction (EBSD) using a JEOL-7001F equipped with an orientation imaging microscopy system. EBSD measurements were performed at constant scanning steps of 100 nm, at an acceleration voltage of 30 kV and beam probe currents up to 9 nA. The surface of the samples was prepared for EBSD measurements following a conventional metallographic polishing method using a succession of 6 μm, 3 μm and 1 μm diamond paste and finishing with a final colloidal silica stage. Thereafter, the samples were ion etched using a Gatan Ion Beam PECS system at 1.7 keV and 30μA.

Table 1. Microstructural parameters for the studied materials.

Grade	Wt.% binder	d_{WC} (μm)	C_{WC}	λ_{binder} (μm)
11CoM	11%Co	1.12	0.38	0.42
10CoC	10%Co	2.33	0.31	0.68
15CoM	15%Co	1.15	0.30	0.55
15CoC	15%Co	1.70	0.27	0.77
10CoNiM	8%Co-2%Ni	1.04	0.41	0.36
10CoNiC	8%Co-2%Ni	1.44	0.38	0.47
15CoNiM	12%Co-3%Ni	1.26	0.29	0.60
15CoNiC	12%Co-3%Ni	1.50	0.28	0.68

3. RESULTS AND DISCUSSION

The hardness, TRS, Weibull modulus and fracture toughness of the investigated materials are listed in **Table 2**. As previously reported [18], experimental results indicate that CoNi-base hardmetals exhibit slightly lower hardness and higher toughness values

than Co-based grades (**Figure 1**). A clear influence of the binder chemical nature on the TRS was not evidenced. The flexural strength dispersion evidenced is fairly small for all studied materials; and accordingly, the corresponding Weibull analysis yields high values, indicative of high reliability from a structural viewpoint.

Table 2. Hardness and fracture toughness for the materials investigated.

Grade	HV30 (GPa)	TRS (MPa)	Weibull modulus	K_{Ic} (MPa√m)
11CoM	12.8	3101	36	13.9
10CoC	11.4	2489	35	15.8
15CoM	11.2	2912	39	15.2
15CoC	10.2	2570	54	17.0
10CoNiM	12.3	2720	23	14.2
10CoNiC	11.6	2534	32	15.3
15CoNiM	10.2	2634	33	15.8
15CoNiC	9.45	2716	31	17.3

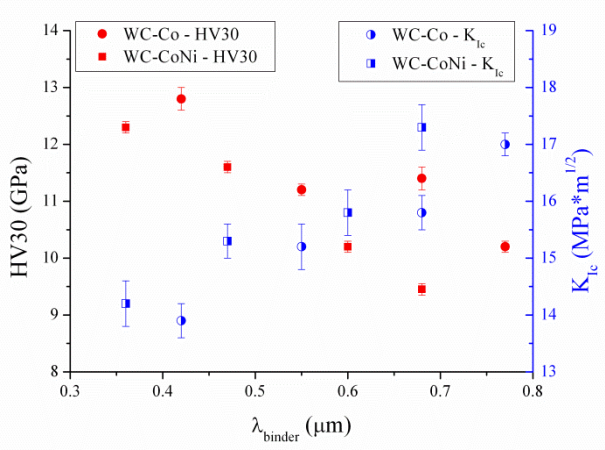

Figure 1. Hardness (left) and fracture toughness (right) values for studied materials.

The FCG curves were measured for the studied materials at two different load ratios: 0.1 and 0.5. FCG thresholds, defined at crack growth rates of 10^{-9} m/cycle, were attained following an incremental loading sequence. **Table 3** shows the determined fatigue threshold and fatigue sensitivity ($1-K_{th}/K_{Ic}$) levels of the studied grades. It is found that coarse-grained materials exhibit a superior fatigue threshold level than medium-grained ones. This improvement is related to a more effective crack-deflection (e.g. **Figure 2**) in large grains, and the fact that it is operative under both monotonic and cyclic loading, i.e. its toughening role is not inhibited or degraded by fatigue. In **Figure 3** the FCG threshold is plotted as a function of the mean grain size for the investigated cemented carbides, together with the data reported in previous studies for a load ratio of 0.1 [9,16,19] for a binder content ranging from 3 to 18 wt.%. It is found that the fatigue threshold correlates the mean grain size through a linear regression of equation

$$K_{th} = 5.75 + 1.27 * d_{WC} \qquad (1)$$

In order to better understand the effects of carbide mean grain size on the crack deflection mechanism, the geometry of the fatigue crack path was characterized by measuring two parameters (**Figure 4**):

- Linear roughness [20], given by

$$R_L = \frac{\sum_1^n L_n}{L_T} \qquad (2)$$

- Weighted mean deflected angle

$$\alpha_m = \frac{\sum_1^n L_n * \alpha_n}{\sum_1^n L_n} \qquad (3)$$

Table 3. FCG threshold and fatigue sensitivity for the studied materials.

Grade	K_{th} (MPa√m)		$1-K_{th}/K_{Ic}$	
	R=0.1	R=0.5	R=0.1	R=0.5
11CoM	7.6	8.6	0.45	0.38
10CoC	8.3	10.4	0.47	0.34
15CoM	7.6	9.1	0.50	0.40
15CoC	8.5	9.6	0.50	0.44
10CoNiM	7.8	9.0	0.45	0.37
10CoNiC	8.0	9.7	0.48	0.37
15CoNiM	7.7	9.6	0.51	0.39
15CoNiC	7.9	9.8	0.54	0.43

The corresponding analyzed fatigue crack growth path regions were propagated at applied K_{max} values slightly above the FCG threshold (i.e. between 7.5 and 10 MPa√m) and over 200 crack segments were measured per grade. The R_L and α_m values obtained for the investigated grades are plotted against the mean grain size in **Figure 5**. The quantified fracture parameters exhibit a linear dependence on the mean grain size with a coefficient of determination of 0.84 and 0.85 for α_m and R_L, respectively. This results proof that the improved fatigue threshold levels obtained for coarse-grained cemented carbides are associated with an increase of the crack deflected angle, which results in a larger effective distance covered by the crack.

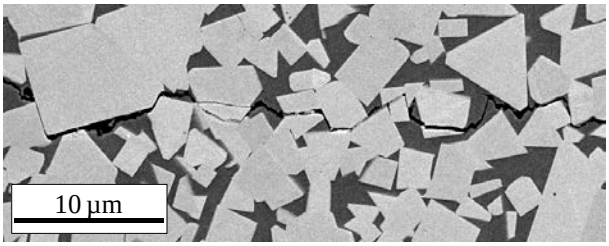

Figure 2. Fatigue crack growth path for the investigated 15CoC cemented carbide.

Llanes et al. [9] investigated the dependence of the fatigue sensitivity of WC-Co hardmetals on their binder

mean free path and applied load ratio. The corresponding proposed trends are plotted in **Figure 6,** together with the fatigue sensitivity exhibited by the studied cemented carbides. According to above comments, the coarse-grained cemented carbides here investigated exhibit lower fatigue sensitivity than expected for WC-Co cemented carbides with alike binder mean free path. Main reason for it is the higher relevance of crack deflection mechanism as microstructure gets coarser. Otherwise, fatigue sensitivity of Co and CoNi base cemented carbides follow similar trends. These results are in accordance with a recent study on the FCG of a WC-Ni hardmetal that report similar fatigue sensitivity values for Nickel and Cobalt base hardmetals [21]. Thus, it appears that Co and CoNi binders exhibit a similar mechanical degradation as toughening agents in cemented carbides when submitted to cyclic loads. This seems to be the case, even though the nature of the binder plastic deformation mechanisms shift from fcc-hcp transformation to slip plus twinning, as the Ni content in the binder increases [22]. In this regard, it is interesting to highlight that plastic deformation mechanisms in the Ni binder include slip and twinning [22,23], also discerned in the Co-base binders, but not stress-induced phase transformation, as it is the case in WC-Co grades.

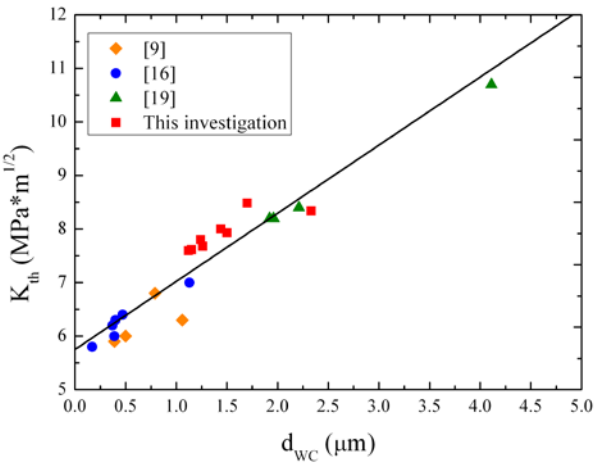

Figure 3. Fatigue threshold as a function of the mean grain size.

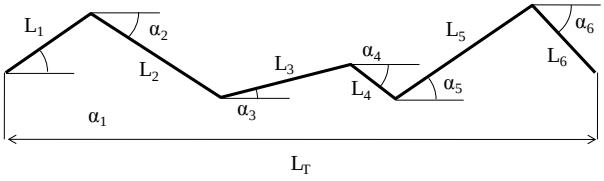

Figure 4. Fatigue crack growth path for the investigated 15CoC cemented carbide.

A crystallographic stable crack growth path within the binder has been evidenced independent of the binder chemical nature (e.g. **Figure 2**). Although the existence of this crystallographic-like paths is documented (e.g. [24,25]), the nature of the fatigue micromechanisms associated with them is not still clear [24]. A recent investigation rationalizes this step-like structure on the basis of an extremely cyclic plastic zone at the crack tip [21].

In order to discern the damage micromechanism within the binder in the vicinity of the crack path a detailed characterization of the fracture path by EBSD was attempted for the 15CoC grade. This particular grade was selected because its large binder mean free path limits the shadowing effect in binder pools and results in high indexing percentages of the binder [26]. Corresponding EBSD maps are shown in **Figure 7**. The maps were produced with a step size of 0.1μm and at a 30kV voltage.

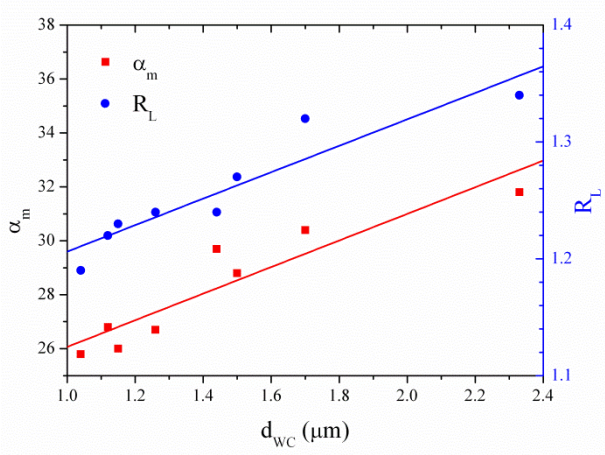

Figure 5. Weighted mean deflected angle (left) and linear roughness (right) for the studied materials.

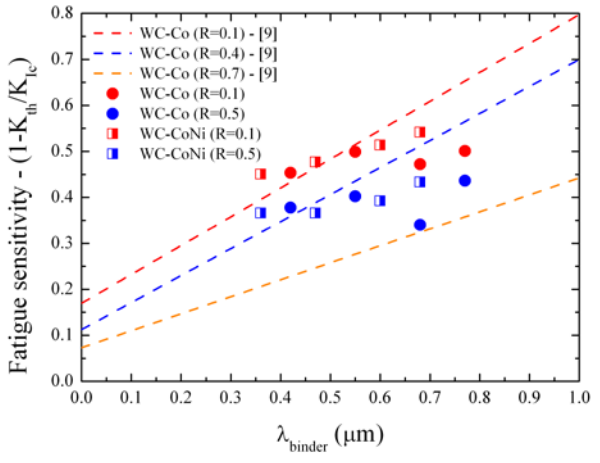

Figure 6. Fatigue sensitivity as a function of binder mean free path for the hardmetals here studied and for the WC-Co grades investigated by Llanes et al. (dashed lines) [9].

Figure 7a shows the WC grains in grey and the fcc and hcp Co phases in red and blue, respectively. Results show a predominance of the hcp phase with and hcp/fcc

ratio of 1.65. This ratio depends on a large number of factors (e.g. solute content, cooling rate, plastic strain induced after cooling and the size of the physical domains [26]). **Figures 7b** and **c** represent the local crystallographic orientations of the fcc and hcp cobalt, respectively. As previously reported, the fcc cobalt forms large grains of about two orders of magnitude the carbide size [25], and the hcp Co nucleates during cooling from the fcc phase in the form of thin lamellas, whose orientation is based on the fcc orientation [27]. In general, no evidence of twinning was found in **Figure 7b** in the vicinity of the crack. On the other hand, no significant increase in hexagonal Co phase in the path of the crack is appreciated (**Figure 7c**). However, it must be stated that the indexing in the crack path is not satisfactory due to its high roughness level. Within this context, the results here presented should be considered as preliminary as further improvement in the preparation of the samples is required in order to increase the indexing ratios.

4. CONCLUSIONS

The FCG behavior of WC-Co and WC-CoNi cemented carbides was investigated. Based on the obtained data the following conclusions may be drawn:

1. FCG threshold of cemented carbides linearly rises when increasing carbide mean grain size, due to a more effective action of the crack deflection mechanism. Therefore, coarse-grained hardmetals are found to be less fatigue sensitive than finer-graded with alike binder mean free path.

2. Co and CoNi binders exhibit a similar mechanical degradation as toughening agents in cemented carbides when submitted to cyclic loads. This is the case, although plastic deformation mechanisms shift from the fcc-hcp transformation to slip plus twinning as the Ni content in the binder increases.

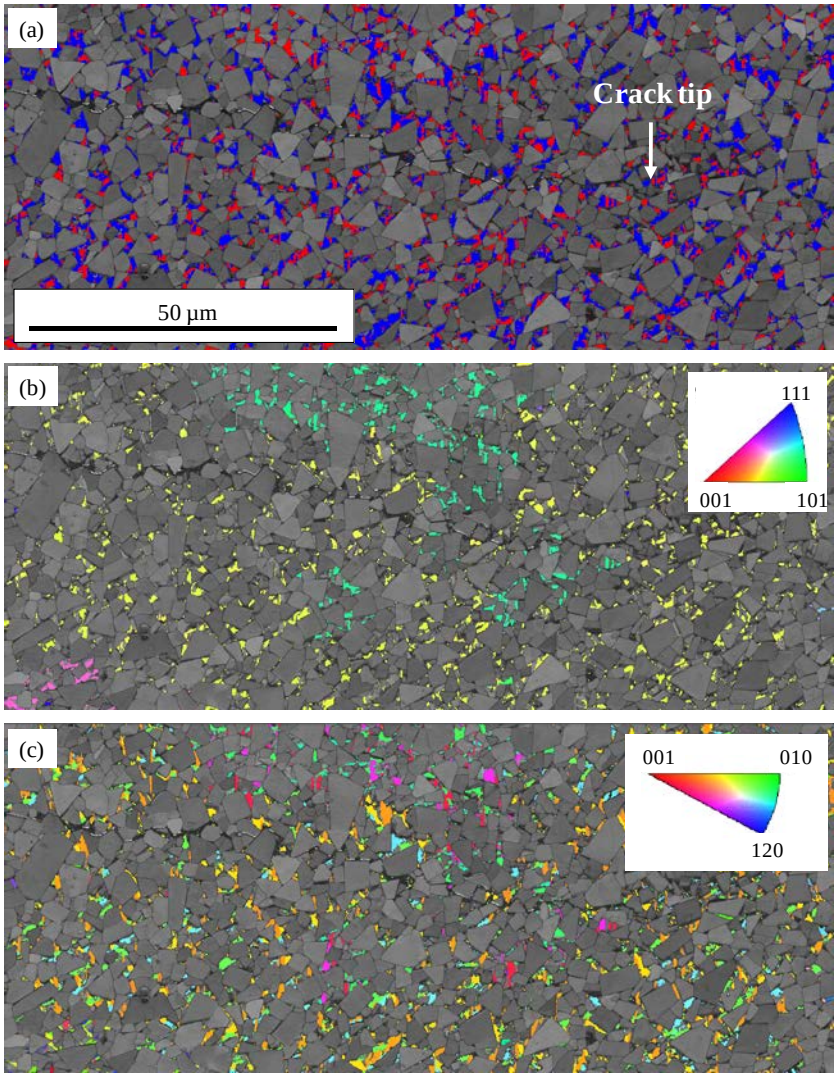

Figure 7. EBSD maps of the fatigue crack path for the 15CoC investigated material corresponding to: (a) Quality image and Phases map containing Co fcc (red) and Co hcp (blue), and local crystallographic orientation for Co fcc (b) and Co hcp (c).

ACKNOWLEDGEMENTS

This work was financially supported by the Spanish Ministerio de Economía y Competitividad (Grant MAT2012-34602). Additionally, J.M. Tarragó acknowledges the Ph.D. scholarship received from the collaborative Industry-University program between Sandvik Hard Materials and Universitat Politècnica de Catalunya.

REFERENCES

[1] Norgren S, Garcia J, Blomqvist A, Yin L. *Global Trends in the Hard Metals Industry, in: Proceedings of the 18th Plansee Seminar*. Reutte: Plansee Group; 2013.

[2] Brookes K. *Metal Powder Report 2011*;66:36.

[3] Dawihl W. *Stahl u Eisen* 1941;61:909.

[4] Schleinkofer U, Sockel HG, Gorting K, Heinrich W. *Materials Science and Engineering A* 1996;209: 103.

[5] Schleinkofer U, Sockel HG, Gorting K, Heinrich W. *Materials Science and Engineering A* 1996;209:313.

[6] Schleinkofer U, Sockel HG, Görting K, Heinrich W. *International Journal of Refractory Metals and Hard Materials* 1997;15:103.

[7] Kursawe S, Pott P, Sockel HG, Heinrich W, Wolf M. *International Journal of Refractory Metals and Hard Materials* 2001;19:335.

[8] Torres Y, Anglada M, Llanes L. *International Journal of Refractory Metals and Hard Materials* 2001;19:341.

[9] Llanes L, Torres Y, Anglada M. *Acta Materialia* 2002;50:2381.

[10] Torres Y, Anglada M, Llanes L. *Fatigue limit - Fatigue crack growth threshold correlation for hardmetals: Influence of microstructure, in: Blom AF (Ed.). Proceedings of the 8th International Fatigue Congress,* EMAS. Stockholm: 2002.

[11] Sailer T, Herr M, Sockel H-G, Schulte R, Feld H, Prakash LJ. *International Journal of Refractory Metals and Hard Materials* 2001;19:553.

[12] Torres Y. Ph.D. Thesis. Universitat Politècnica de Catalunya, 2002.

[13] Coureaux D. Ph.D. Thesis. Universitat Politècnica de Catalunya, 2012.

[14] Sigl LS, Fischmeister HF. *Acta Metallurgica et Materialia* 1988;36:887.

[15] Viswanadham RK, Sun TS, Drake EF, Peck J. *Journal of Materials Science 1981*;16:1029.

[16] Roebuck B, Almond EA. *International Materials Reviews 1988*;33:90.

[17] Torres Y, Casellas D, Anglada M, Llanes L. *International Journal of Refractory Metals and Hard Materials 2001*;19:27.

[18] Tracey VA. *International Journal of Refractory Metals and Hard Materials 1992*;11:137.

[19] Sigl LS, Exner HE. *Metallurgical and Materials Transactions A 1987*;18A:1299.

[20] Tarragó JM, Ferrari C, Reig B, Coureaux D, Schneider L, Llanes L. *Fatigue behavior of a WC-Ni cemented carbide, in: Proceedings of the 18th Plansee Seminar*. Reutte: Plansee Group; 2013.

[21] Vasel CH, Krawitz AD, Drake EF, Kenik EA. *Metallurgical and Materials Transactions A* 1985;16A:2309.

[22] Drake EF, Krawitz AD. *Metallurgical and Materials Transactions A* 1981;12A:505.

[23] Erling G, Kursawe S, Luyck S, Sockel HG. *Journal of Materials Science Letters* 2000;19:437.

[24] Tarragó JM, Turón M, Rivero L, Schneider L, Llanes L. *Toughening and fatigue micromechanisms in hardmetals: SEM / FIB tomography characterization, in: Proceedings of the 18th Plansee Seminar*. Reutte: Plansee Group; 2013.

[25] Mingard KP, Roebuck B, Marshall J, Sweetman G. *Acta Materialia* 2011;59:2277.

[26] Roebuck B, Almond EA. *Materials Science and Engineering* 1984;66:179.

[27] Marshall JM, Kusoffsky A. *International Journal of Refractory Metals and Hard Materials* 2013;40:27.